

Surface-Plasmon-Enhanced Third-Order Harmonic Generation of Organic Materials

Fanghui Ren¹, Xiangyu Wang¹, Zhongan Li², Jingdong Luo², Sei-Hum Jang², Alex K-Y Jen², Alan X. Wang^{1*}

¹School of Electrical Engineering and Computer Science, Oregon State University, Corvallis, OR, 97331, USA

²Department of Materials Science and Engineering, the University of Washington, Seattle, WA, 98195, USA

*Corresponding author wang@eecs.oregonstate.edu

ABSTRACT

We design and fabricate metallic photonic crystals that are integrated with highly-efficient third-order nonlinear polymers. Compared with nanoparticle-doped composite materials, metallic photonic crystals are favorable due to the presence of Bragg-grating-modulated surface plasmon polaritons (SPPs) with strong light localization in large spatial volumes to uniformly enhance the harmonic signals. We experimentally observed extraordinary emission of THG signals from the surface-plasmon-enhanced organic thin film using telecommunication wavelength pulsed laser. This hybrid organic-plasmonic nanostructure opens a new avenue to develop innovative nonlinear optical devices.

Keywords: localized surface plasmons. polymer; third harmonic generation; nonlinear optics

1. INTRODUCTION

Extraordinarily large nonlinear effects have been demonstrated at visible wavelength using gold(Au) nanoparticle (NP)-doped composites[1-4]. However, this approach faces two insurmountable challenges at telecom wavelengths: First, gold NPs do not have plasmonic resonances at telecom wavelengths, so the nonlinear enhancement is negligible; Second, metallic NPs-doped composites have strong optical scattering and absorption, which will induce very high optical loss, particularly at the resonant frequency [5]. In this work, we report the optical design, device fabrication, and experimental characterization of an organic-plasmonic hybrid nanostructure based on high-Q Au nano-patch arrays infiltrated with polymethine-based polymer to enhance the third-order harmonic generation (THG). The periodicity of the metallic photonic crystal and the thickness of the polymer film are fine-tuned such that the optical resonances of these two nanostructures will overlap and couple with each other to obtain extraordinary optical transmission and significantly enhanced electric field intensity. High resolution images of THG qualitatively indicate the field enhancement of each individual photonic crystal pixel.

2. THEORETICAL INVESTIGATION

The sketch of the device configuration is shown in Fig. 1(a), which consists of 2-D arrays of Au patches on top of a glass substrate. The top layer is the nonlinear polycarbonate composite films doped with 50 wt% AJBC 1725, which acts as the nonlinear medium to provide THG effect in the experiment. The geometric dimensions are shown in Fig. 1(a), where the periodicities $p_x=p_y=891$ nm, and the gap size between any two adjacent patches $g=100$ nm. Simulations were conducted based on a three-dimensional (3D) finite element method using the RF module within Comsol 3.5a. The electrical field enhancement and the optical transmission were theoretically investigated. A periodic boundary condition was applied in the simulation. A plane wave was used as the excitation light with electric field polarized along the x-axis. The SPP wavelength (λ_{spp}) is determined by the permittivities of the polymer (ϵ_d) and Au (ϵ_{Au}), and the periodicity of the grating (p_x and p_y). The refractive index of the polymer AJBC measured by an ellipsometer is 1.8. At the near infrared wavelengths from 1400 nm to 1700 nm, a strongly asymmetric Fano resonance centered at 1543 nm was observed from the simulated wavelength range, as shown in Fig. 2(a). The resonance with a sharp bandgap was attributed to the discrete guided modes induced by the Bragg-grating-modulated SPPs couple to the broadband resonance in the narrow slits [6-7]. A plasmonic bandgap was formed from the transmission spectrum, which shows as the minimum transmission state at

1558 nm. From the transmission spectrum, the Q-factor was determined as high as 257, indicating that the 2-D nano-patch plasmonic structure could act as a suitable resonator for telecommunication system. Figure 2(b) and Figure 2(c) are the cross-sectional view and top view of the intensity distribution $|E/E_0|^2$ (where E_0 is the peak electric field of the incident light) associated with the SPPs at the Au-polymer interface at 1543 nm respectively. Enhanced electric fields are located over the surface of the gold patch, and the maximum enhancement factor of intensity $|E/E_0|^2$ is as high as 46. In a typical nano-plasmonic system, the field localization of a nano-antenna usually concentrates in a “hot spot” with the volume of a few cubic nanometers in the gap region, which limits the overall enhancement [8-9]. However, the concentrated electric field in the 2D Au nanopatch array covers nearly entire Au patch surface and extends deeply into the polymer layer, resulting in a relatively uniform electric field enhancement over a large volume.

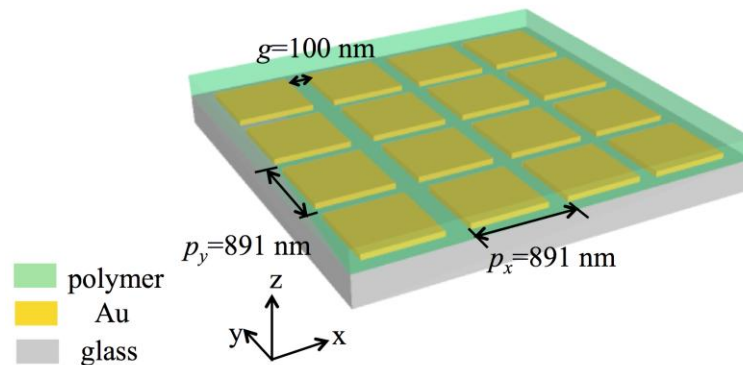


Figure 1 Sketch of the 2D gold nano-patch arrays on a glass substrate. The top layer is the nonlinear polycarbonate composite films doped with 50 wt% AJBC 1725.

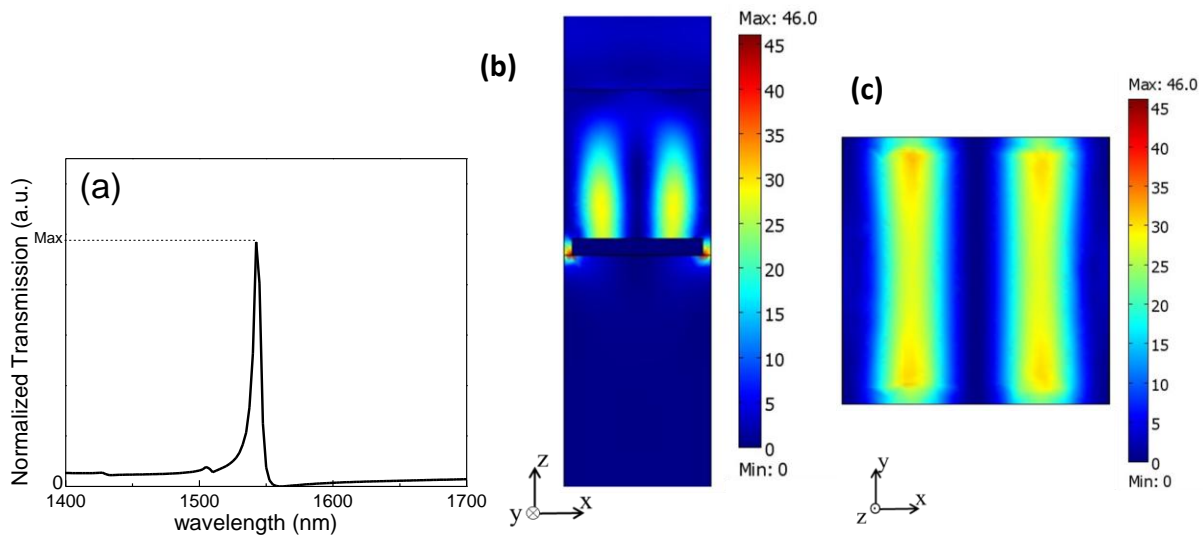


Figure 2 (a) The simulated transmission spectrum. The electric field distribution of 2D periodic gold arrays for normally incident x-polarized E-field (b) from the cross-sectional view (c) from the top view.

3. EXPERIMENTAL RESULTS

Polymer AJBC 1725 was synthesized and optimized by blending anionic polymethine salts and polycarbonate, which enables excellent third order nonlinear susceptibility, low optical loss, and excellent optical power handling capability. The third-order susceptibilities $\chi^{(3)}$ was found to be three times larger than that of silicon at 1550 nm [10]. Figure 3(a) shows the photograph of a spin-coated polymer thin film on a glass cover slide with thickness of 1 μm . A 100 nm Au thin film was deposited onto the glass substrate by thermal evaporation, followed by a focused-ion beam (FIB) lithography process to mill the nano-slit arrays. The periodicity of the fabricated device well matched the designed parameter and variation gap width was controlled less than 5%. A scanning electron microscopy (SEM) image of the 2-D nano-patch arrays after the FIB milling is shown in Fig. 3(c), which indicates the highly ordered 2-D arrays of nano-

patch with rounded corner less than 15 nm. A thin film of polymer with thickness of 1 μm was spin-coated on top of the Au layer to form a hybrid organic-plasmonic structure. The optical image of the polymer-on-grating device after fabrication is shown in Fig. 3(b). In order to compare the THG efficiency, a control device was fabricated, which was 1 μm polymer on top of a 100 nm Au thin film without patterning any plasmonic structure.

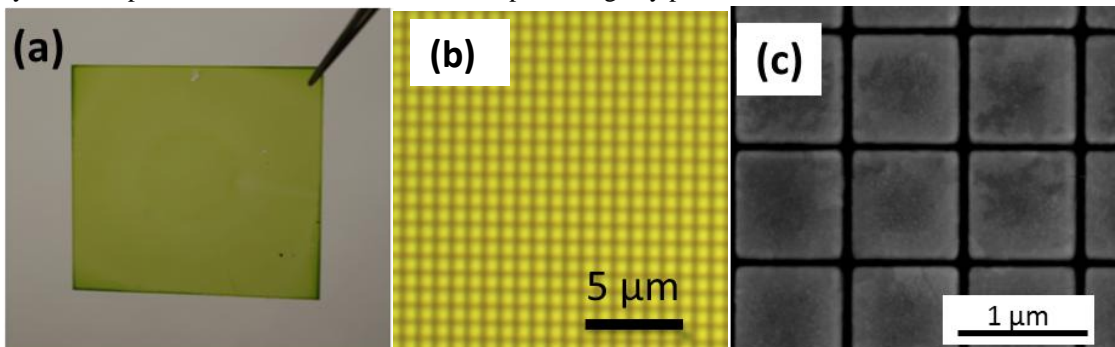


Figure 3. (a) A representative photograph of the nonlinear polymer thin film on a glass substrate. (b) The optical image of the plasmonic structure under bright field microscope. (c) The SEM image of the plasmonic structure after FIB process, showing highly ordered nano-patch arrays

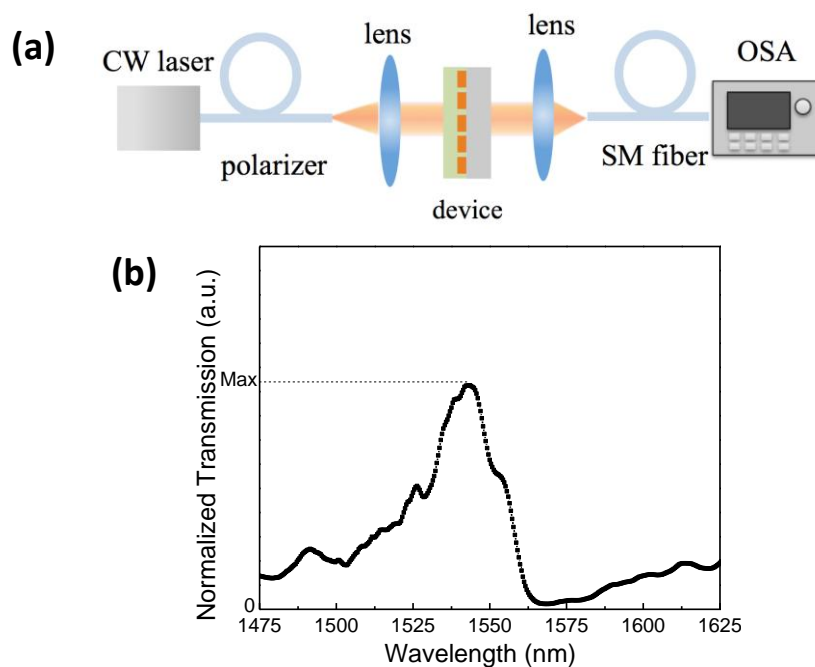


Figure 4. (a) the experimental setup for transmission spectrum measurement (SM:single mode, CW: constant wave, OSA: optical spectrum analyzer) (b) The transmission spectrum of the device.

Figure 4(a) shows the experimental setup for measurement of transmission spectrum. A broadband constant wave laser (Thorlab S5FC1550S) from 1.5-1.6 μm wavelength was used to launch the light centered at 1550 nm, which was coupled into a fiber-based polarizer, resulting in a linearly polarized light. The output light was then collimated by a 40 \times objective lens (NA=0.65). The transmitted beam after the sample was focused by a 40 \times objective lens and coupled into a standard SMF-28 fiber and measured by an HP 70951A Optical Spectrum Analyzer. From the transmission spectrum in Fig. 4(b), an asymmetric Fano resonance is shown on the measured wavelength range, of which the resonant peak is centered at 1543 nm with full width half maximum of 22 nm. Therefore, the measurement showed a Q-factor of 70.1,

which is reduced compared with simulation results mentioned previously. The enlarged bandgap of the Fano resonance and the reduced Q-factor are attributed to the fabrication defects and the imperfect beam collimation.

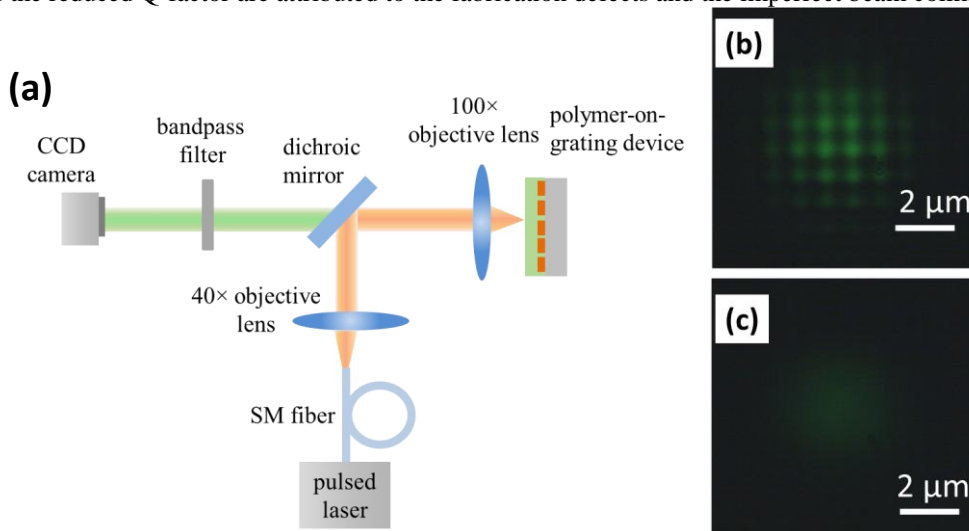


Figure 5(a) the experimental setup of imaging the THG signal from the devices. (b) The captured THG from the organic-plasmonic structure (c) The captured THG from polymer without plasmonic structure

The experimental setup for the observation of THG from the organic-plasmonic device is shown in Fig. 5(a). A fiber-based femtosecond laser (Calmar Laser, FPL-03CFF) was launched to pump the polymer-Au hybrid plasmonic device with a repetition frequency of 20 MHz. The output light was collimated by a 40× objective lens (NA=0.65). A dichroic mirror was used to reflect the pump laser centered at 1550 nm, while allowing the transmission of the THG wavelengths centered at 517 nm. The reflected beam was focused by a 100× objective lens (NA=0.90). The polymer-on-grating sample was mounted at the focal plane of the objective lens on a three-dimensional translation stage. After focusing, the spot size diameter of the pump laser was approximately 8 μm. Due to the excitation of SPPs at the polymer-Au interface, the emission of the THG from the polymer (at frequency $\omega_{THG} = 3\omega$) was significantly enhanced. The THG emission was imaged by a colored CCD camera (Thorlabs, DCC1645C) in the far field after filtering the pump laser using a bandpass filter (Thorlabs, FB520-10). The captured high-resolution images from the CCD in Fig. 5(b) and Fig. 5(c) qualitatively compare the THG emission from the polymer with the plasmonic structures (2D grating) and polymer without the plasmonic structure. The qualitative comparison indicates that the polymer with plasmonic structure shows much greater THG efficiency ($\eta = I_{THG}/I_{pump}$), which is due to the electric field enhancement of the surface plasmon resonance at the organic-plasmonic structure.

4. CONCLUSION

In conclusion, we designed and fabricated a plasmonic nanostructure to enhance the THG efficiency from polymer at telecom wavelengths at 1550 nm. Numerical simulation shows that the 2D plasmonic structure demonstrates a large-volume optical field enhancement throughout the bulk polymer. Optical transmission measurement shows that extraordinary transmission of the device with Q factor as high as 70.1. Polymer with plasmonic structure shows greater THG emission compared with that without plasmonic structure due to the electric field localization at the SPP resonant wavelengths. This organic-plasmonic hybrid nanostructure has great potential for the future application for all-optical signal processing devices.

REFERENCES

- [1] Palomba, S., Danckwerts, M., and Novotny, L., "Nonlinear plasmonics with gold nanoparticle antennas", *J. Opt. A: Pure Appl. Opt.*, 11, 114030(2009).
- [2] Wenseleers, W., Stellacci, F., Meyer-Friedrichsen, T., Mangel, T., Bauer, C. A., Pond, S. JK, Marder, S. R., and Perry, J. W., "Five Orders-of-Magnitude Enhancement of Two-Photon Absorption for Dyes on Silver Nanoparticle Fractal Clusters", *J. Phys. Chem. B*, 106, 6853-6863(2002).
- [3] Cohanoschi, I., and Hernández. F. E., "Surface plasmon enhancement of two-and three-photon absorption of Hoechst 33 258 dye in activated gold colloid solution", *J. Phys. Chem. B*, 109, 14506-14512(2005).
- [4] Liao, H. B., Xiao, R. F., Wang, H., Wong, K. S., and Wong, G. K. L., "Large third-order optical nonlinearity in Au: TiO₂ composite films measured on a femtosecond time scale", *Appl. Phys. Lett.* 72, 1817-1819(1998).
- [5] Ung, T., Liz-Marzán, L. M., and Mulvaney, P., "Optical properties of thin films of Au@SiO₂ particles," *J. Phys. Chem. B* 105, 3441-3452 (2001)
- [6] Luk'yanchuk, B., Zheludev, N. I., Maier, S. A., Halas, N. J., Nordlander, P., Giessen, H., and Chong, C. T., "The Fano resonance in plasmonic nanostructures and metamaterials." *Nature Mater.*, 9, 707-715(2010).
- [7] Christ, A., Zentgraf, T., Kuhl, J., Tikhodeev, S. G., Gippius, N. A., and Giessen, H., "Optical properties of planar metallic photonic crystal structures: Experiment and theory", *Phys. Rev. B*, 70, 125113(2004).
- [8] Bakker, R. M., Boltasseva, A., Liu, Z., Pedersen, R. H., Gresillon, S., Kildishev, A. V., Drachev, V. P., and Shalaev., V. M., "Near-field excitation of nanoantenna resonance", *Opt. Express*, 15, 13682-13688(2007).
- [9] Wustholz, K. L., Henry, A. I., McMahon, J. M., Freeman, R. G., Valley, N., Piotti, M. E., Natan, M. J. , Schatz, G. C., and Van Duyne, R. P., "Structure-activity relationships in gold nanoparticle dimers and trimers for surface-enhanced Raman spectroscopy." *J. Am. Chem. Soc.*, 132(31), 10903-10910(2010).
- [10] Li, Z. A., Liu, Y., Kim, H., Hales, J. M., Jang, S. H., Luo, J., Jones T. B., Hochberg, M., Marder., S. R., Perry, J. W., and Jen, A. K. Y., "High-optical-quality blends of anionic polymethine salts and polycarbonate with enhanced third-order non-linearities for silicon-organic hybrid devices", *Adv. Mater.*, 24(44), OP326-OP330 (2012).